

# Downregulation of DAB2IP results in cell proliferation and invasion and contributes to unfavorable outcomes in bladder cancer

Yi-Jun Shen,<sup>1,2</sup> Zhao-Lu Kong,<sup>3</sup> Fang-Ning Wan,<sup>1,2</sup> Hong-Kai Wang,<sup>1,2</sup> Xiao-Jie Bian,<sup>1,2</sup> Hua-Lei Gan,<sup>2,4</sup> Chao-Fu Wang<sup>2,4</sup> and Ding-Wei Ye<sup>1,2</sup>

<sup>1</sup>Department of Urology, Fudan University Shanghai Cancer Center, Shanghai; <sup>2</sup>Department of Oncology, Shanghai Medical College, Fudan University, Shanghai; <sup>3</sup>Institute of Radiation Medicine, Fudan University, Shanghai; <sup>4</sup>Department of Pathology, Fudan University Shanghai Cancer Center, Shanghai, China

## Key words

Biomarker, DAB2IP, prognosis, radical cystectomy, urothelial carcinoma of the bladder

## Correspondence

Ding-Wei Ye, Department of Urology, Fudan University Shanghai Cancer Center, 270 Dong An Road, Shanghai 200032, China.

Tel: +86-21-64175590; Fax: +86-21-64438640;  
E-mail: dwyeli@163.com

## Funding Information

National Nature Science Foundation of China (31270896).  
Shanghai Municipal Natural Science Foundation (13ZR1407600 and 11ZR1402100).

Received November 25, 2013; Revised March 27, 2014;  
Accepted March 28, 2014

Cancer Sci 105 (2014) 704–712

doi: 10.1111/cas.12407

The DOC-2/DAB2 interactive protein (DAB2IP) is a member of the Ras GTPase-activating protein family. It has been shown to be often downregulated and a poor prognostic factor in several human malignancies. In this study, we analyzed the clinicopathological features and outcomes of DAB2IP expression in 135 patients with urothelial carcinoma of the bladder (UCB) treated by radical cystectomy plus bilateral lymph node dissection, and evaluated the effect of DAB2IP knockdown *in vitro* using the MTT method, colony formation assay, cell cycle assay, and cell migration and invasive assay. We found low expression of DAB2IP was significantly associated with high pathological stage ( $P = 0.002$ ), high pathological grade ( $P = 0.02$ ), tumor size more than 3 cm ( $P = 0.04$ ), and presence of histological variants ( $P = 0.01$ ). DAB2IP was an independent prognostic factor of disease recurrence (hazard ratio, 2.67;  $P = 0.034$ ) and cancer-specific survival (hazard ratio, 2.79;  $P = 0.038$ ). Knockdown of DAB2IP could promote cell proliferation, migration, and invasion. Downregulation of DAB2IP could activate the ERK and Akt pathways and was correlated with the expression of epithelial–mesenchymal transition markers, such as E-cadherin and vimentin. In conclusion, downregulation of DAB2IP is associated with features of biologically aggressive UCB and results in cell proliferation, migration, and invasion of bladder cancer. DAB2IP may serve as a promising biomarker in patients with UCB treated by radical cystectomy and bilateral lymph node dissection.

Bladder cancer is one of the most common malignancies worldwide with an estimated 386 300 new cases and 150 200 deaths in 2008.<sup>(1)</sup> Urothelial carcinoma of the bladder accounts for 90% of all bladder cancer, and is divided into two distinct forms with different prognosis: non-muscle-invasive bladder cancer, which is frequently recurrent and can sometimes become invasive, and MIBC, 50% of which will develop distant metastasis after radical cystectomy plus bilateral lymph node dissection within 2 years.<sup>(2)</sup> Despite advances in surgical techniques and improvement of perioperative chemotherapy, the outcome of MIBC remains poor. Hence, there is a great need for novel prognostic biomarkers and possible novel therapeutic targets to improve clinical management of UCB.

DOC-2/DAB2 interacting protein, also named apoptosis signal-regulating kinase-interacting protein 1, is a novel member of the Ras GTPase-activating protein family.<sup>(3)</sup> The N-terminal domain of DAB2IP interacts with DIP1/2, a Ras GTPase-activating protein, then forms a unique protein complex with a negative regulatory activity that modulates the Ras-mediated signaling pathway.<sup>(4)</sup> DAB2IP has been implicated in cell proliferation, apoptosis, survival, and metastasis of cancer cells through inhibition of the Ras–ERK pathway,

activation of the ASK1–JNK pathway, inhibition of the PI3K–Akt pathway, and EMT, respectively.<sup>(4–7)</sup> Due to the altered epigenetic regulation, such as DNA methylation and histone modification in the *DAB2IP* promoter region, downregulation of DAB2IP was found in different human malignancies including prostate cancer, breast cancer, lung cancer, hepatocellular carcinoma, pancreatic cancer, gastrointestinal tumor, and medulloblastoma.<sup>(8–14)</sup> Moreover, it was shown that downregulation of DAB2IP was resistant to ionizing radiation<sup>(15)</sup> and contributed to a poor prognosis in several types of malignancies.<sup>(11,14,16)</sup> All the above data suggests that DAB2IP may function as a tumor suppressive protein and could be a prognostic factor in cancer.

However, the expression and biological function of DAB2IP in UCB has not yet been explored. In this study, we first investigated the expression of DAB2IP in UCB and assessed its prognostic value in patients treated with RC plus bilateral lymphadenectomy. Second, we determined the effect of DAB2IP knockdown on cell proliferation, cell cycle distribution, cell migration, and invasion *in vitro*. Finally, we studied the possible molecular pathway involved in the development and progression of UCB.

## Materials and Methods

**Patients, tissue samples, and cell lines.** A total of 135 patients treated with RC and bilateral lymphadenectomy for UCB between 2003 and 2011 at Fudan University Shanghai Cancer Center (Shanghai, China) were enrolled in this study. An additional 30 cases (21 for normal bladder urothelium and 9 for inflammatory bladder urothelium), from non-UCB patients who underwent bladder biopsy for non-neoplastic condition, were included as controls. Indications for RC were muscle-invasive disease or recurrent Ta, T1, or carcinoma *in situ* refractory to transurethral resection with or without intravesical chemo- or immunotherapy. None of the patients had any history of systemic chemotherapy or radiotherapy before surgery. None of the patients had known metastatic disease at the time of surgery as shown by radiographic and/or nuclear imaging. A total of 33 (24.4%) patients received adjuvant chemotherapy within 3 months after surgery based on their tumor stage, lymph node status, and overall health status. The study was carried out after receiving approval by a local human investigations committee.

All primary UCB samples were fixed in 10% formalin, embedded in paraffin, sectioned consecutively at 4  $\mu$ m, and stained by H&E. Tumor grade was assigned according to the 2004 World Health Organization/International Society of Urologic Pathology classification and the pathologic stage was assigned according to the 2002 American Joint Committee on Cancer TNM staging system.

Two bladder urothelial cancer cell lines (T24 and 5637) purchased from ATCC (Rockville, MD, USA) were maintained in RPMI-1640 medium (high glucose; HyClone, Beijing, China) supplemented with 10% FBS (Invitrogen, Shanghai, China), 100 U/mL penicillin, and 100  $\mu$ g/mL streptomycin at 37°C, 5% CO<sub>2</sub>, and 95% humidity.

**Immunohistochemistry and scoring.** The sections were deparaffinized and rehydrated, and endogenous peroxidase was blocked with 1.0% H<sub>2</sub>O<sub>2</sub> diluted in PBS. For antigen retrieval, slides were boiled in 10 mM sodium citrate buffer (pH 6.0) for 3.5 min in a microwave oven on high power and another 5 min on low power. After blocking with 5% normal goat serum for 30 min, primary DAB2IP polyclonal antibody (1:50, gift from Prof. J. T. Hsieh) as well as Tp53, Ki67, E-cadherin, and vimentin polyclonal antibody (all 1:100; Santa Cruz Biotechnology, Santa Cruz, CA, USA) in blocking buffer were applied and the slides were incubated overnight at 4°C. After incubation with biotinylated goat anti-rabbit secondary antibody for 1 h, biotinyl-tyramide working solution for 10 min, and streptavidin-HRP (from Tyramide Signal Amplification kit) for 30 min, the visualization signal was developed with DAB. The stained tissue sections were reviewed and scored separately by two pathologists blinded to the clinical parameters. Discordant cases were discussed around a double-headed microscope in order to obtain a consensus classification.

The total DAB2IP immunostaining scoring was calculated as the sum of the percent positivity of stained tumor cells and the staining intensity according to previous published reports.<sup>(11)</sup> The percent positivity was scored as: 0, for 0%; 1, 1–25%; 2, 26–50%; 3, 51–75%; and 4, >75%. The staining intensity was scored as: 0, no staining; 1, weakly stained; 2, moderately stained; and 3, strongly stained. Both percent positivity of cells and staining intensity were decided in a double blinded manner. The staining of DAB2IP was assessed as: –, a final staining score of <3; +, a final staining score of 3; ++, a final staining score of 4; and +++, a final staining score of  $\geq$ 5.

Kaplan–Meier analyses revealed that low expression of DAB2IP (final staining score of – or +) or high expression of DAB2IP (final staining score of ++ or +++) was the best discriminator for disease recurrence and cancer-specific survival. Tp53 immunoreactivity was considered positive when samples showed at least 10% nuclear reactivity.<sup>(17)</sup> Ki67 immunoreactivity was considered positive when samples showed >10% nuclear reactivity.<sup>(17)</sup>

**RNA interference.** Transient inhibition of human DAB2IP was carried out by transfection with 20 nM DAB2IP siRNA (siRIP1-A, 5'-GGA GCG CAA CAG UUA CCU GTT-3'; siRIP1-B, 5'-GGU GAA GGA CUU CCU GAC ATT-3'; siRIP1-C, 5'-GGA CUU GUU UUU UGU CAC ATT-3'), or control siRNA (5'-CTG GAC TTC CAG AAG AAC A-3')<sup>(5)</sup> using Lipofectamine 2000 (Invitrogen) according to the manufacturer's instructions. All siRNA oligonucleotides were synthesized by Genepharma (Shanghai, China).

**Western blot analyses.** Cell lysates were prepared from each sample with a lysis buffer (50 mM Tris, pH 7.5, 1% NP-40, 1 mM EDTA) and a cocktail of protease and phosphatase inhibitors (1 mM Phenylmethanesulfonyl fluoride, 0.2 mM sodium orthovanadate, 0.1 mM sodium fluoride, 10  $\mu$ g/mL aprotinin, and 10  $\mu$ g/mL leupeptin). The supernatant was collected and the protein concentration was quantified by Bradford assay (BioRad, Hercules, CA, USA). An equal amount of total protein (20  $\mu$ g) was subjected to 10% SDS-PAGE and transferred to PVDF membranes for 90 min at 100 V. Membranes were immunoblotted overnight at 4°C with DAB2IP polyclonal antibody (gift from Prof. J.T. Hsieh), phospho-ERK1/2 (T202/Y204), phospho-AKT (Ser473), total ERK1/2, total AKT, and actin antibody (all from Cell Signaling Technologies, Beverly, MA, USA), followed by secondary antibodies. Signals were detected by enhanced chemiluminescence (Pierce, Rockford, IL, USA).

**Cell proliferation assay.** Exponentially growing cells were trypsinized and counted using a particle counter (Beckman Coulter, Fullerton, CA, USA). The cells were then seeded in 96-well plates ( $1 \times 10^3$  cells/mL) with 100  $\mu$ L cell suspension in each well and incubated for 7 days. Then MTT was added to a final concentration of 0.5 mg/mL (Promega, Madison, WI, USA) in the well and the plates were incubated for 4 h at 37°C. Removed medium and formazan crystals were solubilized by adding 150  $\mu$ L DMSO. The absorbance value of each well was measured with a microplate reader set at 570 nm. Each experiment was repeated three times.

**Colony formation assay.** Approximately  $1 \times 10^3$  cells were added to each well of a 6-well culture plate. The cells were incubated at 37°C for 10 days, then were washed twice with PBS and stained with a mixture of 20% methanol and 0.1% crystal violet for 30 min. The number of colonies containing 50 cells or more was counted under an IX71 inverted microscope (Olympus, Tokyo, Japan).

**Cell cycle assay.** Cells were plated in 100-mm dishes overnight and samples were collected on the second day. Medium was collected to recover floating cells, and attached cells were harvested by trypsinization and mixed with the pool of floating cells. After fixing and propidium iodide staining, samples were analyzed through a flow cytometer (Gallios; Beckman Coulter). Three independent experiments were carried out and at least 20 000 cells were counted, the proportion of cells of different phase was gated and calculated using the software ModFit LT3.1 (Verity Software House, Topsham, ME, USA).

**Migration and invasion assay.** A 24-well plate containing 8-mm pore size chamber inserts (BD Biosciences, San Jose,

CA, USA) was used to evaluate the migration and invasion of tumor cells. For the migration assay,  $5 \times 10^4$  cells were seeded in the upper chamber. For the invasion assay, the membrane was coated with Matrigel to form a matrix barrier, and  $1 \times 10^5$  cells were placed in the upper chamber. In each lower chamber, 800 mL serum-free medium with 10% FBS was added. After several hours of incubation at 37°C, cells that had migrated through the pores were fixed and stained with a mixture of 20% methanol and 0.1% crystal violet for 30 min. The cells were then photographed and counted under an IX71 inverted microscope (Olympus).

**Statistical analysis.** Differences in variables with a continuous distribution across categories were assessed using the *t*-test. Fisher's exact test and the  $\chi^2$ -test were used to evaluate the association between categorical variables. Univariable RFS and CSS probabilities were estimated using the Kaplan–Meier method; differences were assessed using the log–rank test. Multivariable Cox regression models addressed time to recurrence and cancer-specific mortality. *In vitro* proliferation, colony formation, cell cycle, and migration and invasion assays were carried out in triplicate and tested using one-way ANOVA. The data are shown as the mean  $\pm$  standard deviation. All tests are two-sided and a *P*-value of 0.05 was set to be statistically significant. All analyses were carried out using spss 16.0 (SPSS, Chicago, IL, USA).

## Results

**Association of DAB2IP expression with clinicopathologic features of UCB.** Expression of DAB2IP was noted mainly in the cytoplasm of bladder urothelial cells. When positive, intensity of DAB2IP positivity in cells ranged from 1 to 7, and it was diffuse (Fig. 1). Of all UCB tissues, 72.6% (98/135) showed low expression of DAB2IP, whereas only 16.7% (5/30) bladder urothelium controls did ( $\chi^2 = 32.9$ ,  $P < 0.0001$ ; Table 1).

The association of DAB2IP with clinicopathologic features of UCB is shown in Table 2. Low expression of DAB2IP was significantly associated with high tumor stages ( $\chi^2 = 17.185$ ,  $P = 0.002$ ), high tumor grade ( $\chi^2 = 5.112$ ,  $P = 0.024$ ), larger tumor size ( $\chi^2 = 4.193$ ,  $P = 0.041$ ), and presence of histologi-

**Table 1.** Expression of DOC-2/DAB2 interactive protein (DAB2IP) in urothelial carcinoma of the bladder (UCB) tissues and bladder urothelium controls

	DAB2IP expression		<i>P</i> -value
	Low	High	
Normal bladder urothelium	3	18	<0.0001
Inflammatory bladder urothelium	2	7	
UCB	98	37	

cal variants ( $\chi^2 = 6.553$ ,  $P = 0.01$ ). Although not statistically significant, 28.6% (28/98) of patients with low expression of DAB2IP had lymph node metastasis compared with 13.5% (5/37) patients with high expression of DAB2IP ( $\chi^2 = 3.297$ ,  $P = 0.069$ ). No significant associations were found between DAB2IP expression and age, gender, lymphovascular invasion, adjuvant chemotherapy, or the expression of Tp53 and Ki67 ( $P > 0.05$ ).

**Association of DAB2IP expression with clinical outcomes.** Median follow-up for patients was 46 months. Disease recurred in 51 patients (37.8%), and 46 (34.1%) died of UCB. Actuarial RFS estimates at 3 and 5 years were  $66.8 \pm 4.2\%$  (standard error) and  $61.0 \pm 4.6\%$ , respectively. Actuarial CSS estimates at 3 and 5 years were  $74.7 \pm 4\%$  and  $66.8 \pm 4.5\%$ , respectively. The Kaplan–Meier analysis and the log–rank test showed that the expression of DAB2IP was associated with an increased risk of disease recurrence ( $P < 0.001$ ) and cancer-specific mortality ( $P < 0.001$ ) in UCB patients who underwent RC plus bilateral lymphadenectomy (Fig. 2).

Univariate Cox proportional hazards analysis of RFS and CSS showed that DAB2IP and other established prognostic factors including age, tumor stage, grade, size, lymph node invasion, histological variants, lymphovascular invasion, receipt of adjuvant chemotherapy, and expression of Tp53 and Ki67 were all significant risk factors for recurrence and death due to UCB (Table 3). In multivariate analyses, when controlling for the

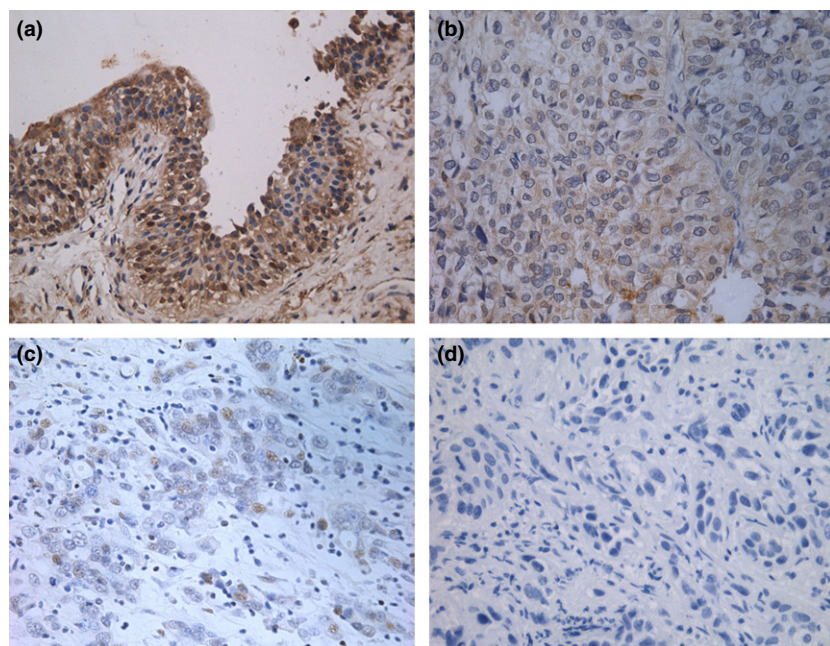


**Fig. 1.** Expression of DOC-2/DAB2 interactive protein (DAB2IP) in urothelial carcinoma of the bladder (UCB) tissues and bladder urothelium controls by immunohistochemistry. (a) High expression of DAB2IP in normal bladder urothelium scored as 7 (magnification,  $\times 200$ ). (b) High expression of DAB2IP in low-grade UCB tissue scored as 5 ( $\times 200$ ). (c) Low expression of DAB2IP in high-grade UCB tissue scored as 2 ( $\times 200$ ). (d) Low expression of DAB2IP in high-grade UCB tissue scored as 0 ( $\times 200$ ).

**Table 2.** Descriptive characteristics of 135 patients treated with radical cystectomy for urothelial carcinoma of the bladder stratified according to DOC-2/DAB2 interactive protein (DAB2IP) expression

	DAB2IP expression		P-value
	Low	High	
Age, years (average)	59.3	57.6	0.380
Gender			
Male	79	30	0.951
Female	19	7	
pT stage			
Ta	4	7	0.002
T1	20	11	
T2	29	11	
T3	31	8	
T4	14	0	
Tumor size			
≤3 cm	39	22	0.041
>3 cm	59	15	
Grade			
Low	23	16	0.024
High	75	21	
LNI			
Negative	70	32	0.069
Positive	28	5	
HV			
No	66	33	0.010
Yes	32	4	
LVI			
No	61	26	0.385
Yes	37	11	
Adjuvant chemotherapy			
No	72	30	0.359
Yes	26	7	
Tp53			
Negative	46	20	0.461
Positive	52	17	
Ki67			
Negative	42	20	0.244
Positive	56	17	

HV, histological variants; LNI, lymph node invasion; LVI, lymphovascular invasion; Tp53, tumor protein p53.

effects of standard clinicopathologic features and molecular markers, the expression of DAB2IP was an independent predictor of RFS (HR, 2.67,  $P = 0.034$ ; Table 3) and CSS (HR, 2.79,  $P = 0.038$ ; Table 4), respectively. Pathologic tumor stage and the expression of Tp53 were also independent predictors of RFS (HR, 2.92,  $P = 0.016$ ; HR, 2.37,  $P = 0.006$ ) and CSS (HR, 3.25,  $P = 0.012$ ; HR, 2.63,  $P = 0.005$ ), respectively.

**Knockdown of DAB2IP increased cell proliferation and S-phase cell distribution.** Endogenous levels of DAB2IP protein in T24 and 5637 were both knocked down using RNAi and confirmed by Western blot analysis (Fig. 3a). Compared to cells transfected with CON-siRNA cells, no obvious change in cell morphology could be observed on DAB2IP-siRNA cells using RNAi (Fig. 3b). However, DAB2IP-siRNA cells grew more quickly than CON-siRNA cells ( $P < 0.05$ ; Fig. 3c,d) accompanied with higher S-phase cell distribution. S-phase percentages for T24 cells: DAB2IP-siRNA versus CON-siRNA,  $47.91 \pm$

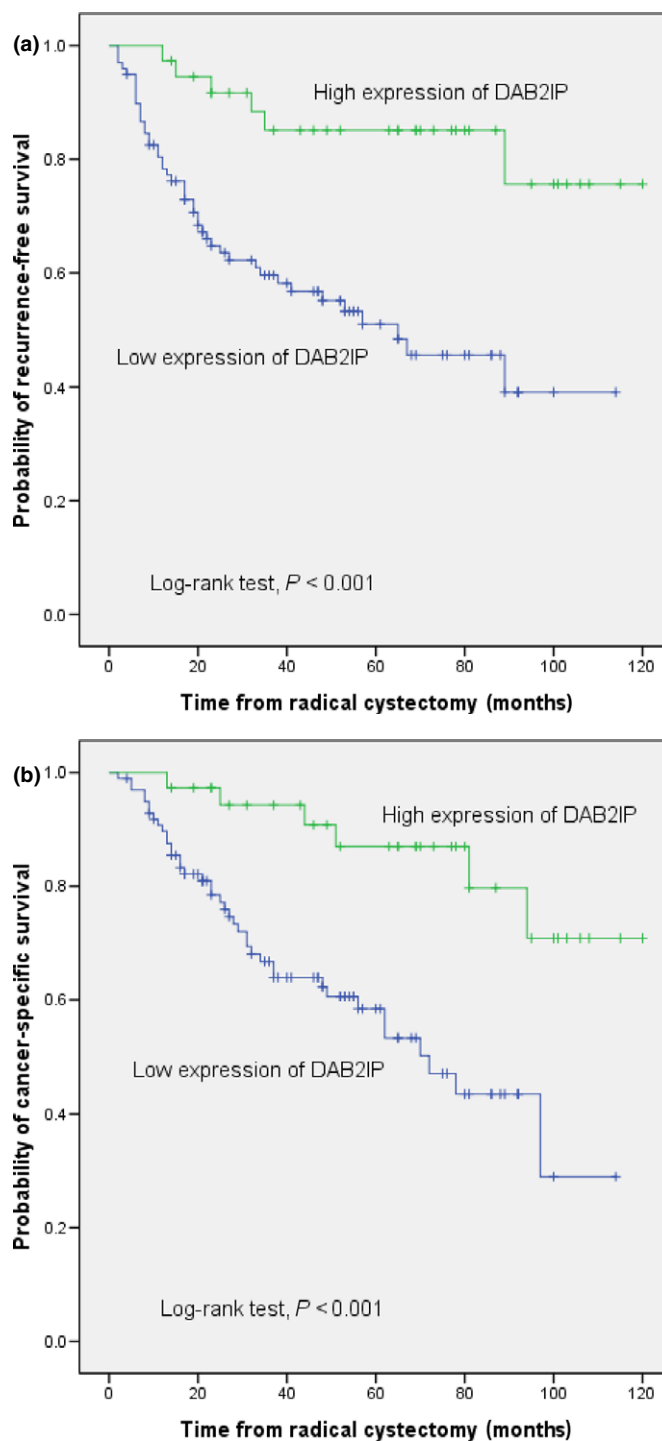


**Fig. 2.** Kaplan–Meier plots of recurrence-free survival (a) and cancer-specific survival (b) estimates in 135 patients with urothelial carcinoma of the bladder treated with radical cystectomy and bilateral lymphadenectomy, stratified by DOC-2/DAB2 interactive protein (DAB2IP) expression.

1.03 versus  $38.40 \pm 0.83$ ,  $P = 0.009$ ; S-phase percentages for 5637 cells: DAB2IP-siRNA versus CON-siRNA,  $53.81 \pm 1.38$  versus  $38.77 \pm 1.14$ ,  $P = 0.007$  (Fig. 3e).

**Knockdown of DAB2IP enhanced cell migration and invasion ability.** Given that DAB2IP inhibits the proliferation of bladder cancer cells, we next studied its function on cell motility. In

**Table 3. Univariate Cox regression analyses of recurrence-free survival and cancer-specific survival in 135 patients with urothelial carcinoma of the bladder treated with radical cystectomy and bilateral lymph node dissection**

Variable	Recurrence-free survival			Cancer-specific survival		
	HR	95% CI	P-value	HR	95% CI	P-value
Age, years (continuous)	1.031	0.999–1.065	0.049	1.040	1.006–1.075	0.022
Gender (male vs female)	1.220	0.573–2.597	0.606	1.255	0.561–2.809	0.581
Tumor size, cm (continuous)	1.151	1.042–1.270	0.005	1.151	1.036–1.278	0.009
pT stage (pT3–4 vs pTa–2)	5.411	2.993–9.783	<0.001	5.950	3.155–11.222	<0.001
Grade (HG vs LG)	2.521	1.272–4.997	0.008	3.252	1.550–6.821	0.002
LNI (positive vs negative)	4.434	2.500–7.865	<0.001	4.751	2.588–8.720	<0.001
HV (positive vs negative)	3.811	2.157–6.732	<0.001	3.713	2.029–6.796	<0.001
LVI (positive vs negative)	2.179	1.251–3.797	0.006	2.172	1.203–3.922	0.010
Receipt of adjuvant chemotherapy (yes vs no)	2.710	1.538–4.776	0.001	2.413	1.320–4.411	0.004
Tp53 (positive vs negative)	3.154	1.703–5.483	<0.001	3.768	1.912–7.427	<0.001
Ki67 (positive vs negative)	2.420	1.336–4.385	0.004	2.378	1.278–4.422	0.006
DAB2IP expression (low vs high)	4.123	1.750–9.713	0.001	4.185	1.745–10.033	0.001

CI, confidence interval; DAB2IP, DOC-2/DAB2 interactive protein; HG, high grade; HR, hazard ratio; HV, histological variants; LG, low grade; LNI, lymph node invasion; LVI, lymphovascular invasion; Tp53, tumor protein p53.

**Table 4. Multivariate Cox regression analyses of recurrence-free survival and cancer-specific survival in 135 patients with urothelial carcinoma of the bladder treated with radical cystectomy and bilateral lymph node dissection**

Variable	Recurrence-free survival			Cancer-specific survival		
	HR	95% CI	P-value	HR	95% CI	P-value
Age, years (continuous)	1.025	0.986–1.067	0.213	1.038	0.995–1.083	0.087
Tumor size, cm (continuous)	1.078	0.959–1.211	0.207	1.083	0.954–1.229	0.217
pT stage (pT3–4 vs pTa–2)	2.920	1.220–6.989	0.016	3.247	1.302–8.100	0.012
Grade (HG vs LG)	1.372	0.567–3.322	0.483	1.146	0.444–2.960	0.778
LNI (positive vs negative)	1.243	0.573–2.695	0.582	1.244	0.553–2.799	0.597
HV (positive vs negative)	1.680	0.826–3.418	0.152	1.344	0.637–2.837	0.438
LVI (positive vs negative)	1.203	0.587–2.463	0.614	1.337	0.618–2.893	0.460
Receipt of adjuvant chemotherapy (yes vs no)	1.380	0.683–2.788	0.369	1.299	0.617–2.734	0.491
Tp53 (positive vs negative)	2.372	1.286–4.377	0.006	2.628	1.345–5.137	0.005
Ki67 (positive vs negative)	1.821	0.937–3.537	0.077	1.643	0.832–3.246	0.153
DAB2IP expression (low vs high)	2.673	1.078–6.630	0.034	2.794	1.059–7.375	0.038

Variables with  $P < 0.05$  in univariate analysis were included in the multivariate analysis. CI, confidence interval; DAB2IP, DOC-2/DAB2 interactive protein; HG, high grade; HR, hazard ratio; HV, histological variants; LG, low grade; LNI, lymph node invasion; LVI, lymphovascular invasion; Tp53, tumor protein p53.

the migration assay, DAB2IP-siRNA cells showed an enhanced migratory ability compared to CON-siRNA cells. For T24 cells: DAB2IP-siRNA versus CON-siRNA,  $160.3 \pm 27.5$  versus  $97.33 \pm 11.2$ ,  $P = 0.02$ ; for 5637 cells: DAB2IP-siRNA versus CON-siRNA,  $283.7 \pm 30.1$  versus  $188.0 \pm 22.5$ ,  $P = 0.01$  (Fig. 4a). Similarly, in the invasion assay, DAB2IP-siRNA cells showed a marked increase in the ability to traverse through the Matrigel-coated membrane. For T24 cells: DAB2IP-siRNA versus CON-siRNA,  $335.0 \pm 21.4$  versus  $242.7 \pm 23.5$ ,  $P = 0.007$ ; for 5637 cells: DAB2IP-siRNA versus CON-siRNA,  $531.7 \pm 36.2$  versus  $299.3 \pm 34.5$ ,  $P = 0.001$  (Fig. 4b).

**Knockdown of DAB2IP led to activation of ERK and Akt.** To reveal the mechanism of DAB2IP function in these events, the activation status of Akt or ERK was determined based on the specific phosphorylation site of each protein. Compared with CON-siRNA cells, a dramatic activation of p-ERK1/2 and p-Akt was detected in DAB2IP-siRNA cells (Fig. 5). These data showed that downregulation of DAB2IP could activate

ERK or Akt in the presence of DAB2IP siRNA to knock down endogenous DAB2IP levels in bladder cancer cell lines.

**Correlation between DAB2IP expression and EMT markers.** We further examined the relationship between DAB2IP expression and EMT markers including E-cadherin and vimentin using human bladder specimens. Low expression of DAB2IP and E-cadherin as well as increased expression of vimentin were clearly detected in tissues from bladder cancer patients (Fig. 6). There was a significant correlation between the levels of DAB2IP and E-cadherin ( $r = 0.817$ ) and an inverse correlation between the levels of DAB2IP and vimentin ( $r = 0.666$ ) in the tested samples (Table 5).

## Discussion

To our knowledge, this is the first study to investigate the expression level and biological function of DAB2IP in UCB. We obtained two major results. First, we found DAB2IP was downregulated in UCB, was strongly correlated with unfavorable

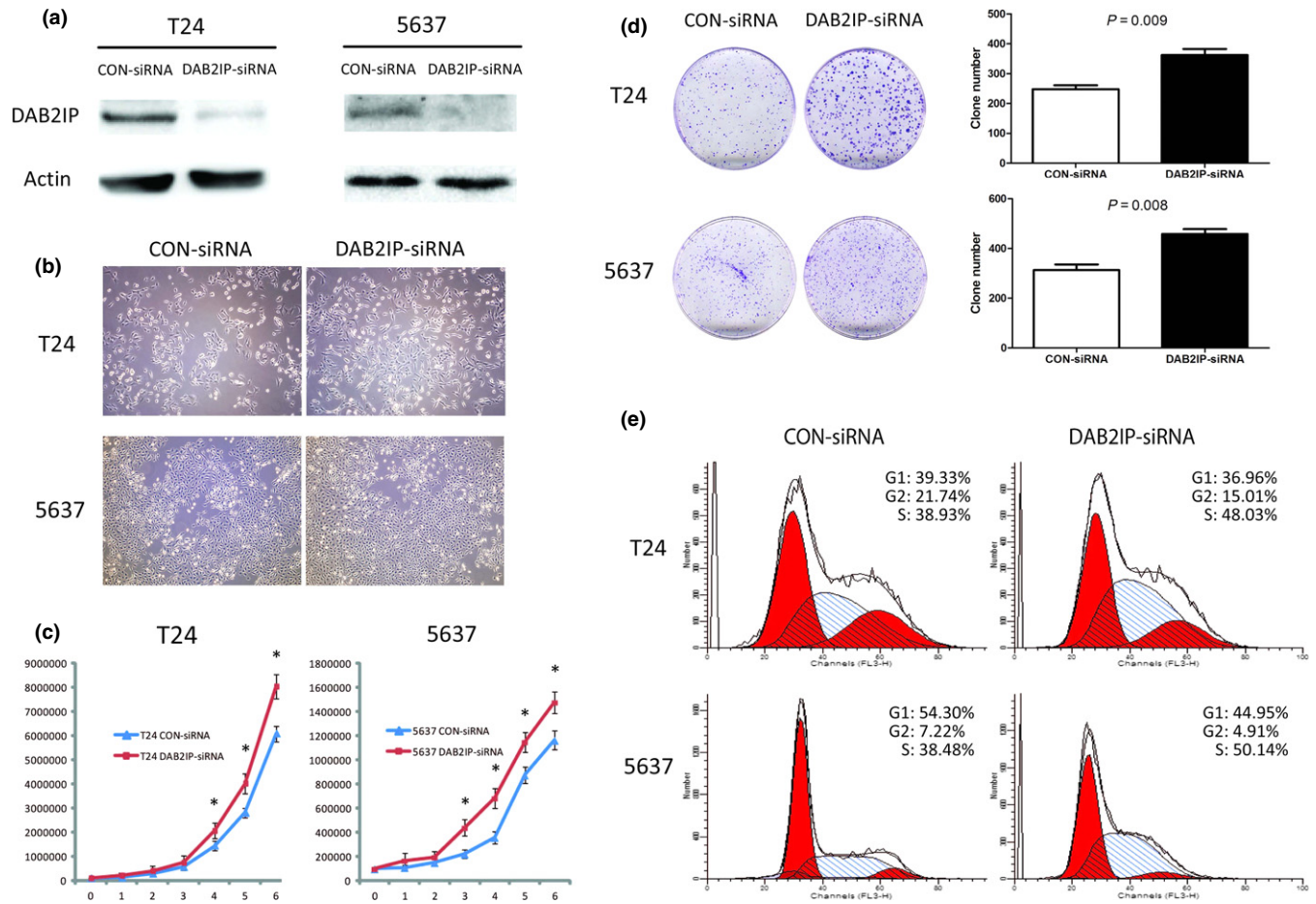


**Fig. 3.** Effects of DOC-2/DAB2 interactive protein (DAB2IP) silencing on cell proliferation and cell cycle *in vitro* of bladder urothelial cancer cells. (a) Knockdown of DAB2IP by specific siRNA was analyzed by Western blot. (b) Effect of DAB2IP depletion on cell morphology in T24 and 5637 cells transfected with specific siRNA (DAB2IP-siRNA) or negative control (CON-siRNA) under an inverted microscope (magnification,  $\times 100$ ). (c) Silencing endogenous DAB2IP promoted cell proliferation, as determined by MTT assay. Each bar represents the mean  $\pm$  SD of three independent experiments.  $*P < 0.05$ . (d) Effect of DAB2IP depletion on the colony formation abilities of T24 and 5637 cells. Representative images are shown on the left, and quantification is shown on the right. The results are representative of three independent experiments, and the values shown are the mean  $\pm$  SD. (e) Knockdown of DAB2IP resulted in more S-phase cell distribution. The population of cells in different phases was assessed by flow cytometric assay with propidium iodide staining and the percentages of cells in each phase are shown at the top right of each graph.

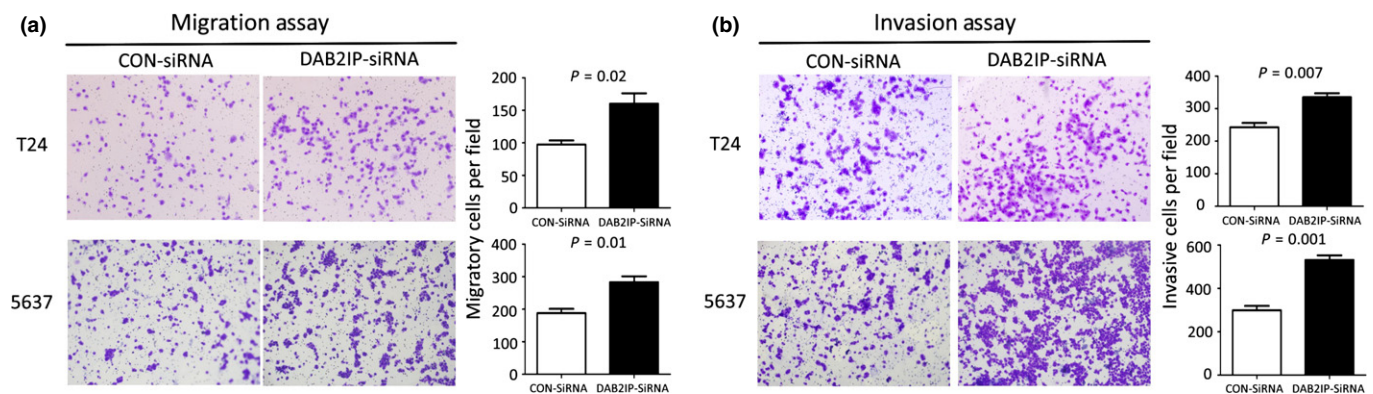


**Fig. 4.** Transwell migration and invasion assays of T24 and 5637 bladder urothelial cancer cells transfected with specific siRNA (DAB2IP-siRNA) or negative control (CON-siRNA). Knockdown of DOC-2/DAB2 interactive protein (DAB2IP) significantly enhanced the abilities of cell migration (a) and invasion (b) in T24 and 5637 cells. Representative images are shown on the left, and quantification is shown on the right. The results are representative of three independent experiments, and the values shown are the mean  $\pm$  SD.

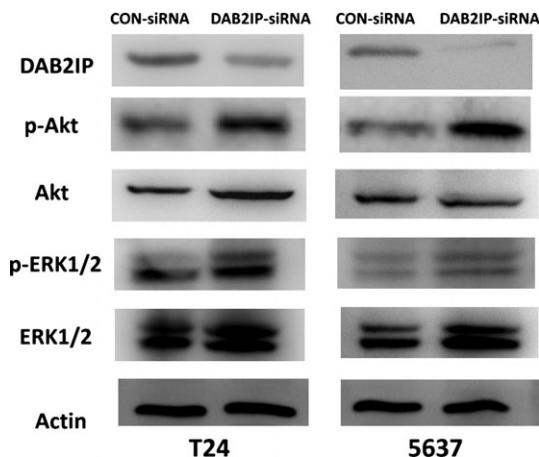


**Fig. 5.** Increased Akt and ERK1/2 activation in T24 and 5637 bladder urothelial cancer cells transfected with specific siRNA (DAB2IP-siRNA) compared to negative control (CON-siRNA). Tissue lysates were analyzed by Western blot using DOC-2/DAB2 interactive protein (DAB2IP), phospho- (p-)Akt (S473), p-ERK1/2 (T202/Y204), total-Akt, and total-ERK1/2. Actin was used as a loading control.

tumor characteristics, and was an independent predictive factor of RFS and CSS in patients treated by RC plus pelvic lymphadenectomy. Second, we observed that DAB2IP suppression resulted in a strongly enhanced cell proliferation, migration, and invasion ability.

In this study, we found nearly three-quarters of UCB tissues showed low expression of DAB2IP whereas only one-sixth of bladder urothelium controls did, which was well in line with studies on other cancer forms, including prostate cancer<sup>(16)</sup> and hepatocellular carcinoma.<sup>(11)</sup> In addition, we found the levels of DAB2IP expression were inversely correlated with tumor stage, tumor grade, tumor size, and presence of histological variants, suggesting that low expression of DAB2IP is a feature of poorly differentiated aggressive tumors.

For bladder cancer, the most reliable known prognostic markers are tumor stage and grade. However, these pathological features are not sufficient to accurately predict the evolution and progression of invasive bladder cancer. The utility and importance of biomarkers has been recognized and may

**Table 5.** Correlation between DOC-2/DAB2 interactive protein (DAB2IP) and E-cadherin (or vimentin) in tissues of 135 patients with urothelial carcinoma of the bladder treated with radical cystectomy and bilateral lymph node dissection

	DAB2IP expression		<i>r</i>	<i>P</i> -value
	Low	High		
E-cadherin				
Low	92	4	0.817	<0.0001
High	6	33		
Vimentin				
Low	15	32	-0.666	<0.0001
High	83	5		

help refine the understanding of the biologic behavior of UCB, thereby improving the risk stratification and clinical management of UCB patients. Our study, for the first time, showed DAB2IP was a promising molecular biomarker for the outcome of UCB, in agreement with previous studies.<sup>(11,16)</sup> To compare with other proven prognostic biomarkers in UCB, we also investigated the prognostic value of Tp53 and Ki67 in this study.<sup>(17,18)</sup> After controlling for the effects of standard clinicopathologic features and molecular markers, tumor stage, Tp53, and DAB2IP were found to be independent prognostic factors for RFS and CSS in patients treated with RC and bilateral lymph node dissection. However, some other key prognostic markers, including histological variants, lymph node invasion, lymphovascular invasion, and Ki67, which had been reported in previous studies,<sup>(19–23)</sup> failed to independently predict the outcome of UCB. This may be because the prognostic markers proven in the present study were more strongly related to UCB outcomes than other prognostic factors. As the meta-analysis clearly indicated a 5% survival advantage of neoadjuvant cisplatin-based chemotherapy in T2–4a N0 UCB patients before local curative therapy,<sup>(24)</sup> identification of patients with high risk of unfavorable outcomes by a biomarker (for example, DAB2IP) may facilitate the use of neoadjuvant chemotherapy as early treatment of metastatic disease while the burden of disease is low.

As low expression of DAB2IP was correlated with unfavorable tumor characteristics and outcomes in UCB, we

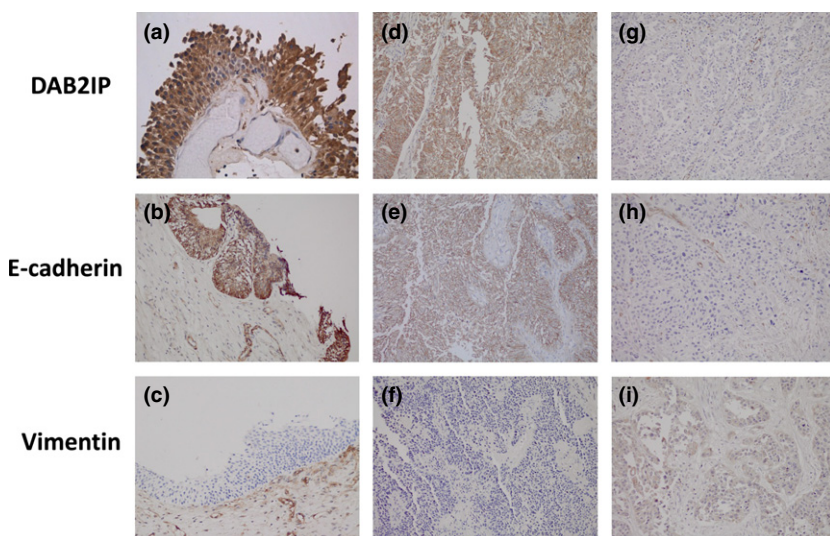


**Fig. 6.** Expression of DOC-2/DAB2 interactive protein (DAB2IP) and epithelial–mesenchymal transition markers in urothelial carcinoma of the bladder (UCB) and normal bladder urothelium by immunohistochemistry. High expression of DAB2IP (a) and E-cadherin (b) but low expression of vimentin (c) is evident in normal bladder urothelium (magnification, ×100). Similarly, high expression of DAB2IP (d) and E-cadherin (e) but low expression of vimentin (f) is evident in low-grade UCB tissue (×100). However, low expression of DAB2IP (g) and E-cadherin (h) but high expression of vimentin (i) is evident in high-grade UCB tissue (×100).

speculated that DAB2IP might be involved in cell proliferation, migration, and invasion. As a result, we found that knockdown of DAB2IP led to a dramatic increase of the proliferation, migration, and invasion ability both in T24 and 5637 cell lines. Both PI3K/Akt and Ras/ERK signaling are well-characterized pathways involved in the control of cell proliferation. These pathways were upregulated in the development and progression of MIBC.<sup>(25)</sup> In the present study, we showed that knockdown of DAB2IP could activate the ERK or Akt pathways *in vitro*. This might partly explain why downregulation of DAB2IP can lead to enhancement of cell proliferation. Epithelial–mesenchymal transition is a critical event of cancer cells that triggers cancer progression; EMT had been found to regulate muscle invasion/metastasis in urothelial cancer.<sup>(26)</sup> Our study also found that expression of DAB2IP was correlated with the expression of EMT markers. This might be one of the reasons why downregulation of DAB2IP resulted in increased cell migration and invasion.

Our study is not devoid of limitations. First and foremost are limitations inherent to the retrospective design and the study's single-centric nature, which may have potential bias in patient selection and changes in treatment strategies over time. Therefore, the predictive value of DAB2IP needs to be validated in multicenter studies prospectively before clinical implementation. The second limitation is the reliability of IHC techniques, which are highly dependent on a range of variables, such as choice of antibody, technical procedures, interpretation, and stratification criteria. We have optimized the DAB2IP IHC protocol in full tissue sections of RC specimens, and can confirm that the protocol in the current study is robust. The third limitation is the lack of a gain-of-function study, that is, to upregulate the endogenous level of DAB2IP in cell lines. As the expression of DAB2IP in T24 and 5637 cells is not

low enough, more bladder cancer cell lines, ideally without endogenous DAB2IP expression, are expected to be tested in future.

To conclude, our results suggest that downregulation of DAB2IP is associated with features of biologically aggressive UCB and results in cell proliferation, migration, and invasion of bladder cancer. DAB2IP may serve as a promising biomarker in patients treated with RC plus bilateral lymph node dissection.

## Acknowledgments

This work was supported by National Nature Science Foundation of China (31270896) and Shanghai Municipal Natural Science Foundation (13ZR1407600 and 11ZR1402100).

## Disclosure Statement

The authors have no conflict of interest.

## Abbreviations

CON-siRNA	control siRNA
CSS	cancer-specific survival
DAB2IP	DOC-2/DAB2 interactive protein
DAB2IP-siRNA	DAB2IP-knockdown
EMT	epithelial–mesenchymal transition
IHC	immunohistochemistry
MIBC	muscle-invasive bladder cancer
RC	radical cystectomy
RFS	recurrence-free survival
TP53	tumor protein p53
UCB	urothelial carcinoma of the bladder

## Reference

- Jemal A, Bray F, Center MM, Ferlay J, Ward E, Forman D. Global cancer statistics. *CA Cancer J Clin* 2011; **61**: 69–90.
- Raghavan D, Shipley WU, Garnick MB, Russell PJ, Richie JP. Biology and management of bladder cancer. *N Engl J Med* 1990 (Apr 19); **322** (16): 1129–38.
- Chen H, Pong RC, Wang Z, Hsieh JT. Differential regulation of the human gene DAB2IP in normal and malignant prostatic epithelia: cloning and characterization. *Genomics* 2002 (Apr); **79** (4): 573–81.
- Wang Z, Tseng CP, Pong RC *et al*. The mechanism of growth-inhibitory effect of DOC-2/DAB2 in prostate cancer. Characterization of a novel GTPase-activating protein associated with N-terminal domain of DOC-2/DAB2. *J Biol Chem* 2002 (Apr 12); **277** (15): 12622–31.
- Xie D, Gore C, Zhou J *et al*. DAB2IP coordinates both PI3K-Akt and ASK1 pathways for cell survival and apoptosis. *Proc Natl Acad Sci U S A* 2009 (Nov 24); **106** (47): 19878–83.
- Zhang H, Zhang R, Luo Y, D'Alessio A, Pober JS, Min W. AIP1/DAB2IP, a novel member of the Ras-GAP family, transduces TRAF2-induced ASK1-JNK activation. *J Biol Chem* 2004 (Oct 22); **279** (43): 44955–65.
- Xie D, Gore C, Liu J *et al*. Role of DAB2IP in modulating epithelial-to-mesenchymal transition and prostate cancer metastasis. *Proc Natl Acad Sci U S A* 2010 (Feb 9); **107** (6): 2485–90.
- Chen H, Toyooka S, Gazdar AF, Hsieh JT. Epigenetic regulation of a novel tumor suppressor gene (hDAB2IP) in prostate cancer cell lines. *J Biol Chem* 2003 (Jan 31); **278** (5): 3121–30.
- Dote H, Toyooka S, Tsukuda K *et al*. Aberrant promoter methylation in human DAB2 interactive protein (hDAB2IP) gene in breast cancer. *Clin Cancer Res* 2004 (Mar 15); **10** (6): 2082–9.
- Yano M, Toyooka S, Tsukuda K *et al*. Aberrant promoter methylation of human DAB2 interactive protein (hDAB2IP) gene in lung cancers. *Int J Cancer* 2005 (Jan 1); **113** (1): 59–66.
- Zhang X, Li N, Li X *et al*. Low expression of DAB2IP contributes to malignant development and poor prognosis in hepatocellular carcinoma. *J Gastroenterol Hepatol* 2012 (Jun); **27** (6): 1117–25.
- Duan YF, Li DF, Liu YH *et al*. Decreased expression of DAB2IP in pancreatic cancer with wild-type KRAS. *Hepatobiliary Pancreat Dis Int* 2013; **12**: 204–9.
- Dote H, Toyooka S, Tsukuda K *et al*. Aberrant promoter methylation in human DAB2 interactive protein (hDAB2IP) gene in gastrointestinal tumour. *Br J Cancer* 2005 (Mar 28); **92** (6): 1117–25.
- Smits M, van Rijn S, Hulleman E *et al*. EZH2-regulated DAB2IP is a medulloblastoma tumor suppressor and a positive marker for survival. *Clin Cancer Res* 2012 (Aug 1); **18** (15): 4048–58.
- Kong Z, Xie D, Boike T *et al*. Downregulation of human DAB2IP gene expression in prostate cancer cells results in resistance to ionizing radiation. *Cancer Res* 2010 (Apr 1); **70** (7): 2829–39.
- Min J, Zaslavsky A, Fedele G *et al*. An oncogene-tumor suppressor cascade drives metastatic prostate cancer by coordinately activating Ras and nuclear factor-kappaB. *Nat Med* 2010; **16**: 286–94.
- Lotan Y, Bagrodia A, Passoni N *et al*. Prospective evaluation of a molecular marker panel for prediction of recurrence and cancer-specific survival after radical cystectomy. *Eur Urol* 2013 (Sep); **64**(3): 465–71.
- George B, Datar RH, Wu L *et al*. p53 gene and protein status: the role of p53 alterations in predicting outcome in patients with bladder cancer. *J Clin Oncol* 2007 (Dec 1); **25**(34): 5352–8.
- Xylinas E, Rink M, Robinson BD *et al*. Impact of histological variants on oncological outcomes of patients with urothelial carcinoma of the bladder treated with radical cystectomy. *Eur J Cancer* 2013 (May); **49** (8): 1889–97.
- Jeong IG, Park J, Song K *et al*. Comparison of 2002 TNM nodal status with lymph node density in node-positive patients after radical cystectomy for bladder cancer: analysis by the number of lymph nodes removed. *Urol Oncol* 2011; **29**: 199–204.
- Stein JP, Lieskovsky G, Cote R *et al*. Radical cystectomy in the treatment of invasive bladder cancer: long-term results in 1,054 patients. *J Clin Oncol* 2001 (Feb 1); **19** (3): 666–75.
- Tarin TV, Power NE, Ehdia B *et al*. Lymph node-positive bladder cancer treated with radical cystectomy and lymphadenectomy: effect of the level of node positivity. *Eur Urol* 2012 (May); **61** (5): 1025–30.



- 23 Tilki D, Shariat SF, Lotan Y *et al.* Lymphovascular invasion is independently associated with bladder cancer recurrence and survival in patients with final stage T1 disease and negative lymph nodes after radical cystectomy. *BJU Int* 2013 (Jun); **111**: 1215–21.
- 24 Advanced Bladder Cancer (ABC) Meta-analysis collaboration. Neoadjuvant chemotherapy in invasive bladder cancer: update of a systematic review and meta-analysis of individual patient data. *Eur Urol* 2005; **48**: 202–5; discussion 205–6.
- 25 Ewald JA, Downs TM, Cetnar JP, Ricke WA. Expression microarray meta-analysis identifies genes associated with Ras/MAPK and related pathways in progression of muscle-invasive bladder transition cell carcinoma. *PLoS ONE* 2013; **8** (2): e55414.
- 26 McConkey DJ, Choi W, Marquis L *et al.* Role of epithelial-to-mesenchymal transition (EMT) in drug sensitivity and metastasis in bladder cancer. *Cancer Metastasis Rev* 2009; **28**: 335–44.